engineering proceedings

Proceeding Paper

Reliability of Smartphone Positioning in Harsh Environment †

Giovanni Cappello [1], Ciro Gioia [2], Antonio Angrisano [3], Silvio Del Pizzo [4], Gabriele Portelli [4] and Salvatore Gaglione [1,4,*]

1 International Ph.D. Programme UNESCO Chair "Environment, Resources and Sustainable Development", Department of Science and Technology, "Parthenope" University of Naples, 80143 Naples, Italy; giovanni.cappello001@studenti.uniparthenope.it
2 Independent Researcher, 21020 Brebbia, Italy; cirogioia@tin.it
3 Department of Engineering, Messina University, 98166 Messina, Italy; angrisanoa@unime.it
4 Department of Science and Technology, "Parthenope" University of Naples, 80143 Naples, Italy; silvio.delpizzo@uniparthenope.it (S.D.P.); gabriele.portelli001@studenti.uniparthenope.it (G.P.)
* Correspondence: salvatore.gaglione@uniparthenope.it
† Presented at the European Navigation Conference 2023, Noordwijk, The Netherlands, 31 May–2 June 2023.

Abstract: Since 2016, it has been possible to record and collect GNSS (Global Navigation Satellite System) raw data on Android devices. This has been a game changer in low-cost device applications. Researchers in the GNSS field have tried to answer new questions regarding Android device positioning performance, the quality of their measurements, positioning techniques that could be applied, and methods to increase the accuracy and the reliability of the PNT (Position Navigation Timing) solution. Several research groups have demonstrated accurate positioning using smartphones while also showing the potential limitations of such devices. In particular, problems related to the GNSS antenna performance have been reported; indeed, in urban scenarios, where users typically operate, the presence of multiple outliers could make the navigation solution inaccurate, if not unfeasible. Hence, techniques useful for verifying the reliability of the navigation solutions have become fundamental. The reliability of the PNT solution provided by smartphones is an open research question. In this study, traditional RAIM (Receiver Autonomous Integrity Monitoring) algorithms were adapted to the case of smartphones. Navigation solution algorithms, including FDE (Fault Detection and Exclusion), were tested using a long data collection made by a smartphone located in a harsh environment in static mode. The performance of the proposed approaches was assessed in terms of horizontal and vertical errors, solution reliability, and residual distribution.

Keywords: RAIM; integrity; smartphone; subset; Forward–Backward; disturbed scenario

check for updates

Citation: Cappello, G.; Gioia, C.; Angrisano, A.; Del Pizzo, S.; Portelli, G.; Gaglione, S. Reliability of Smartphone Positioning in Harsh Environment. *Eng. Proc.* **2023**, *54*, 44. https://doi.org/10.3390/ENC2023-15429

Academic Editors: Tom Willems and Okko Bleeker

Published: 29 October 2023

1. Introduction

The accurate and reliable positioning of low-cost devices is a current challenge in the Global Navigation Satellite System (GNSS) research field due to the low quality of the collected measurements. In particular, smartphones, the principal device of interest of this study, are used in everyday life for personal navigation, which is usually conducted in urban areas, wherein the presence of buildings can limit signal availability and introduce gross errors in observations, leading to unreliable position calculations. However, in 2016, thanks to the release of Android 7 (Nougat), users became able to collect raw GNSS data [1,2], making it possible for researchers to direct their efforts to the enhancements of smartphone positioning. Several research groups have studied and assessed the quality of observations and the positioning performance of different smartphone devices [3–5]. The low-cost receivers and antennas embedded in smartphones constitute the principal limitation to the positional accuracy of such devices, especially in signal-degraded environments where the presence of recurrent multipath phenomena strongly impacts the navigation solution. In such environments, the identification and exclusion of outliers becomes fundamental. A possible solution to this issue is the application of Receiver

Autonomous Integrity Monitoring (RAIM) algorithms. The benefits of these algorithms have been demonstrated in [6,7], and they can play key roles in detecting and excluding blunder-affected measurements. RAIM is a term that includes a family of user algorithms that, by comparing the consistency between measurements, calculate the integrity of the GNSS solution [8]. Thanks to a residual analysis, RAIM algorithms are capable of determining the most probable satellite whose measurement is blunder-affected [8] with a minimum of five visible satellites and to exclude it with a minimum of six visible satellites [9] in case of a single constellation.

RAIM was born out of aeronautics applications [9,10], but it has also been used in other fields, such as personal navigation [11,12]. The objective of this study was to apply classical RAIM algorithms to smartphone GNSS observables in order to detect and exclude faulty measurements and guarantee the reliability of the navigation solution. Specifically, two Fault Detection and Exclusion (FDE) algorithms were tested: Forward–Backward and Subset.

The integrity algorithm has been tested using real data in a typical signal-degraded scenario. The device adopted for this study was a Xiaomi Mi8 equipped with a Broadcom BCM47755 dual-frequency chip and able to acquire L1/E1 and L5/E5 GNSS signal frequencies [13]. For the proposed study, the introduced device was located in an obstructed environment using an ad hoc setup.

The performances of Single Point Positioning (SPP) with and without the application of RAIM are assessed in terms of horizontal and vertical error, availability (without RAIM), and reliable availability (with RAIM) percentage and residual distribution.

The remainder of this paper is structured as follows: Section 2 details the fundamentals of the SPP technique and RAIM algorithms and provides a brief overview on the main differences between the two adopted algorithms. Section 3 describes the conducted experiment. Section 4 discusses the results, and Section 5 concludes the paper.

2. Positioning and Integrity

SPP is a basic technique largely employed in the satellite navigation field. It enables one to estimate the position of a receiver exploiting pseudorange measurements, the classical equation of which is reported in (1):

$$\rho = d + c\delta t_r + \epsilon \tag{1}$$

where ρ is the pseudorange, d is the satellite-receiver geometrical distance, $c\delta t_r$ is the receiver clock offset (δt_r) (expressed in meters by multiplying it with the speed of light c), ϵ is a term that contains modeled (atmospheric, relativistic, satellite clock errors) and unmodeled errors (multipath, receiver hardware, noise).

Equations such as (1) are linearized around a set of n unknown parameters (whose number varies according to the number of the involved GNSSs), and through acquiring m measurements, the linearized equations can be expressed in a matrix notation as:

$$\underline{z} = H\underline{\Delta x} + \underline{\varepsilon} \tag{2}$$

where $\underline{z}$ represents the vector containing the m differences between observed and corrected pseudoranges (referred to as measurement vector), H is the $m \times n$ design matrix, $\underline{\Delta x}$ is the unknown vector containing the corrections needed to update the position estimated at the previous step, $\underline{\varepsilon}$ is the vector containing the unmodeled errors.

$\underline{\Delta x}$ is estimated using Weighted Least Squares (WLS) [9,14], the solution of which is reported in (3):

$$\underline{\Delta x} = \left(H^T W H\right)^{-1} H^T W \underline{z} \tag{3}$$

where W is the weighting matrix containing diagonal elements that are the inverse of the variance of each measure and whose determination is dependent on the adopted weighting strategy, which, in this work, is based on User Range Accuracy (URA), a parameter provided in the navigation message, and the satellite elevation.

The principal limitation of Single Point Positioning pertains to the reachable accuracy, which, in nominal conditions, is on the metric order [9]. In disturbed environments, where multipath phenomena are frequent events and the satellite visibility is limited, such accuracy can be worsened because the position could be computed considering blunder-affected measurements. In order to guarantee the integrity of the solution, the use of RAIM algorithms is necessary in critical environments in order to detect and eventually exclude erroneous measurements that lead to an inaccurate position. So, after the solution estimation, residuals are analyzed using the RAIM algorithm in order to perform "fault detection" to verify the presence of anomalous measurements and, with sufficient redundancy, "fault exclusion". Classical RAIM algorithms perform, as a first step, a Global Test (GT) that is based on the use of a decision variable D depending on the residual r and the weighting matrix W:

$$\begin{aligned} \underline{r} &= \underline{z} - H\underline{\Delta x} \\ D &= \underline{r}^T W \underline{r} \end{aligned} \tag{4}$$

D is compared with a threshold T, whose values depend on the required performance of RAIM, on the redundancy, and on the assumed behavior of D. If $D > T$, a probable outlier presence is assumed. So, in function of the adopted RAIM algorithms, a Local Test (LT) wherein the standardized residuals $\underline{w}$ are analyzed can be carried out:

$$w_i = \left| \frac{r_i}{\sqrt{CV_{ii}}} \right| \tag{5}$$

where CV_{ii} refers to the respective diagonal elements of the covariance matrix of the residuals. w_i is compared to a local threshold, and the largest one overpassing the threshold is assumed to be a blunder and excluded after a separability check. In the separability check, a coefficient based on the variance of the standardized residuals is analyzed and compared to a specific value (0.9 for this study) in order to avoid erroneous exclusions [15–17].

For this study, independently of the RAIM algorithm, a geometry check was performed before and after the application of RAIM using a threshold of 30 for PDOP, 25 for HDOP, and 20 for VDOP in order to declare the solution unreliable if the DOP (Dilution of Precision) conditions are not satisfied and to not perform the FDE process in bad geometrical conditions. Regarding integrity, the geometry can be further analyzed using the ARP method (the Approximate Radial-error Protected method) [14,18]. Furthermore, if the redundancy is not sufficient to perform fault detection, the solution is declared to be impossible to check and RAIM cannot be applied.

In Sections 2.1 and 2.2, the main differences between the RAIM Subset and RAIM Forward–Backward (FB) algorithms are assessed.

2.1. RAIM Subset

The RAIM Subset algorithm only carries out the Global Test. So, if a set of measurements is declared inconsistent, a series of subsets, in all the possible combinations, are re-checked. The subset passing the GT is declared consistent and, through it, the position is re-computed and declared reliable if the geometry check is passed. If any subset passes the GT, the solution is declared unreliable. The principal drawback of this algorithm is its computational heaviness. In fact, a large number of combinations could require a longer time of computation, especially in cases involving a high number of measurements [15–17].

2.2. RAIM Forward–Backward

RAIM FB performs both GT and LT, and it is based on two steps. The first one, referred to as "Forward", carries out the GT, and if the set is declared inconsistent, the LT is performed to identify and, after the separability check, remove erroneous measurements. The Forward step is repeated recursively until no erroneous measurements remain (or until the chosen maximum number of exclusions). If, after those steps, the solution is declared reliable and more than one blunder has been excluded, the second step, referred to as "Backward", is carried out in order to reinclude any measurements excluded in an erroneous way [15–17].

3. Test Setup

For the conducted experiment, about 14 hours of data collected from a Xiaomi Mi8, manufactured by Xiaomi Corporation [19] smartphone was used. The smartphone was equipped with a Broadcom BCM47755 receiver manufactured by Broadcom Inc [20], able to acquire double-frequency (L1 and L5) measurements from GPS, Glonass, Galileo, BeiDou. With SPP being a single-frequency and code-based positioning technique, only pseudorange observations on the first main frequency are used: L1 for GPS and E1 for Galileo. The Android application used to collect raw GNSS data was "rinex ON". The environment surrounding the device was obstructed, as shown in Figure 1, where, in the upper box, the PDOP (Position Dilution of Precision) values are not optimal, especially for the GPS only configuration from 04:41 to 07:01 of UTC time, where the value is within 2 and 6. PDOP is enhanced in the multi-constellation GPS/Galileo configuration, but its evolution in time clearly indicates an obstructed environment. In the lower box, the satellite visibility is reported. A satellite is considered visible only if its SNR is larger than 20 dB-Hz and its elevation is larger than 15 degrees. For GPS, the number of visible satellites varies between 5 and 11; in addition, rapid variation during the entire test and a fall in the last part was observed. For Galileo, the number of tracked satellites is more limited than GPS; indeed, the number of visible satellites was between 1 and 6.

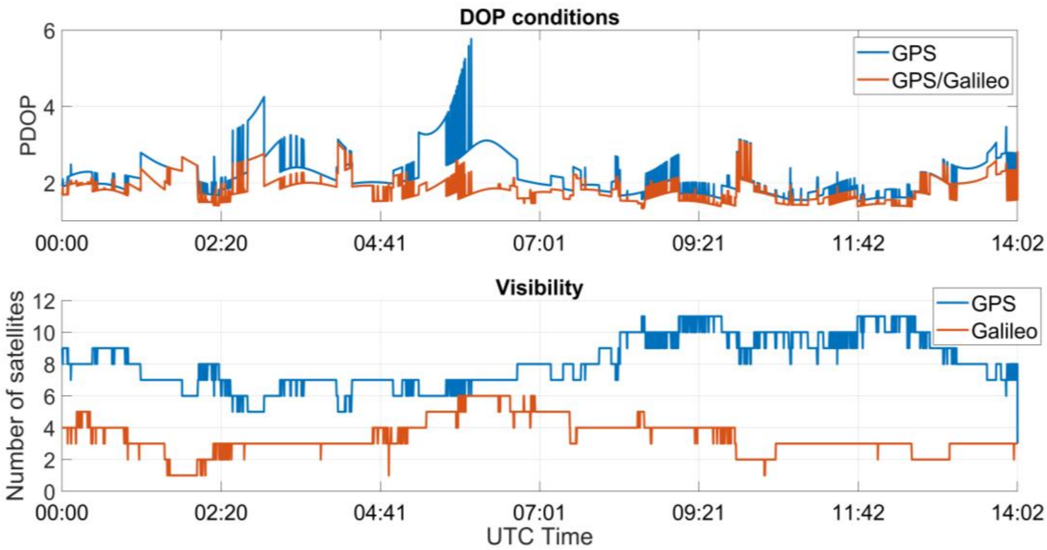

Figure 1. PDOP evolution (**upper box**) and satellite visibility (**lower box**) for the single and double constellation cases.

In Figure 2, the average C/N0 computed for each epoch is shown. From the figure, it can be noted that the parameter has a fast variability, confirming the presence of an obstructed context.

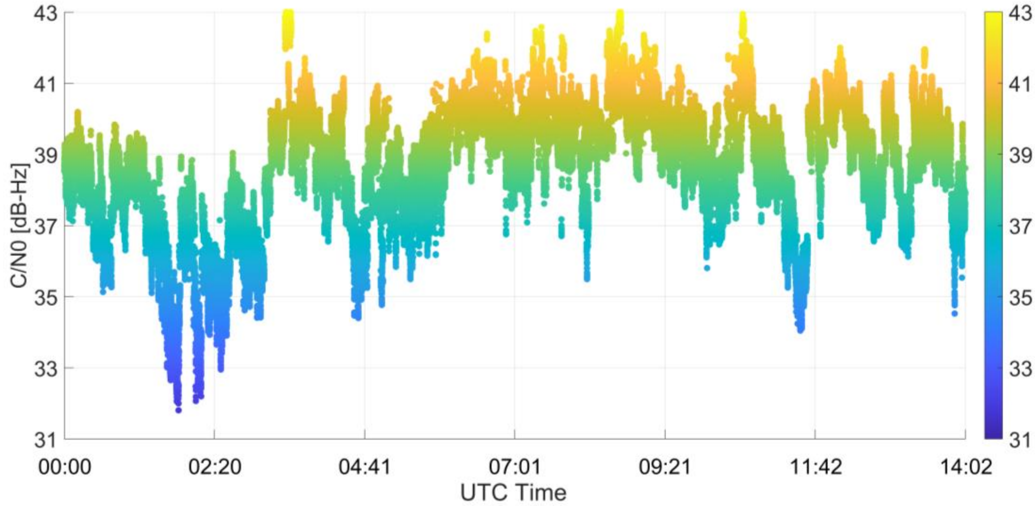

Figure 2. Average C/N0.

4. Results and Discussion

In this section, the results are discussed. The adopted configurations are referred to as "GPS No RAIM" and "GPS/Galileo No RAIM" for cases where RAIM was not applied, "GPS + SS" and "GPS/GAL + SS" for cases where the Subset (SS) algorithm was applied, and "GPS + FB" and "GPS/GAL + FB" for cases where the Forward–Backward (FB) algorithm was applied. Figure 3 shows a horizontal scatter plot for all the considered configurations. From the figure, it can be noted that the configurations with RAIM (yellow markers) have a significant reduction of horizontal errors. In addition, when the integrity algorithms are not able to identify and reject the erroneous measurements, they provide useful information to the user; no trust should be placed in the estimated solution. The unreliable solutions are marked with red markers; for the SS cases, a larger number of unreliable solutions are visible, leading to a decrease in reliability. The 95th percentiles are reported in both figures in black for the "No RAIM" case and in magenta for the "RAIM" case, while their values are reported in Table 1. For all configurations with RAIM, the 95th percentile (computed considering only reliable solutions) is smaller than the no RAIM case. This clearly shows the benefits of the application of the FDE algorithms. For the horizontal channel, the 95th percentile for the SS case is slightly lower than the FB case.

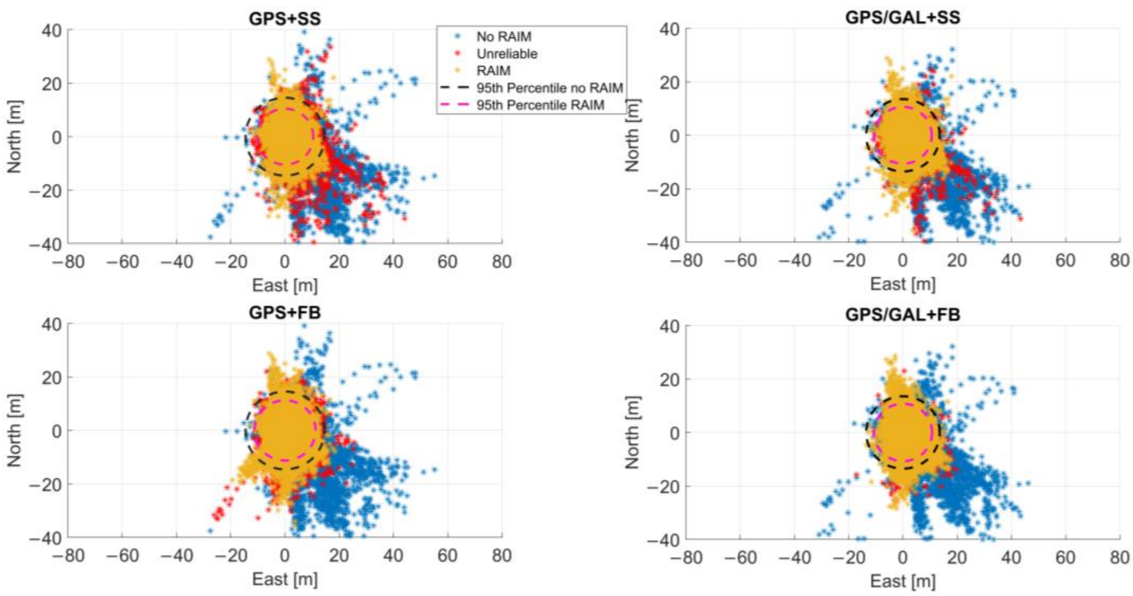

Figure 3. Horizontal scatter plot for all the considered configurations.

Table 1. The 95th Percentile of the horizontal and vertical errors for all the configurations.

Configuration	95th Percentile [m] Horizontal Error	95th Percentile [m] Vertical Error
GPS No RAIM	14.55	22.95
GPS + SS	10.43	17.16
GPS + FB	11.26	18.03
GPS/GAL No RAIM	13.53	19.52
GPS/GAL + SS	10.62	16.07
GPS/GAL + FB	10.74	15.62

In Figure 4, the time evolution of the vertical error for the four configurations is shown. Also, in the vertical channel, the benefits of the application of the FDE techniques are evident. In all the cases, the yellow lines are lower than the blue lines, demonstrating a reduction in the vertical error when RAIM is applied.

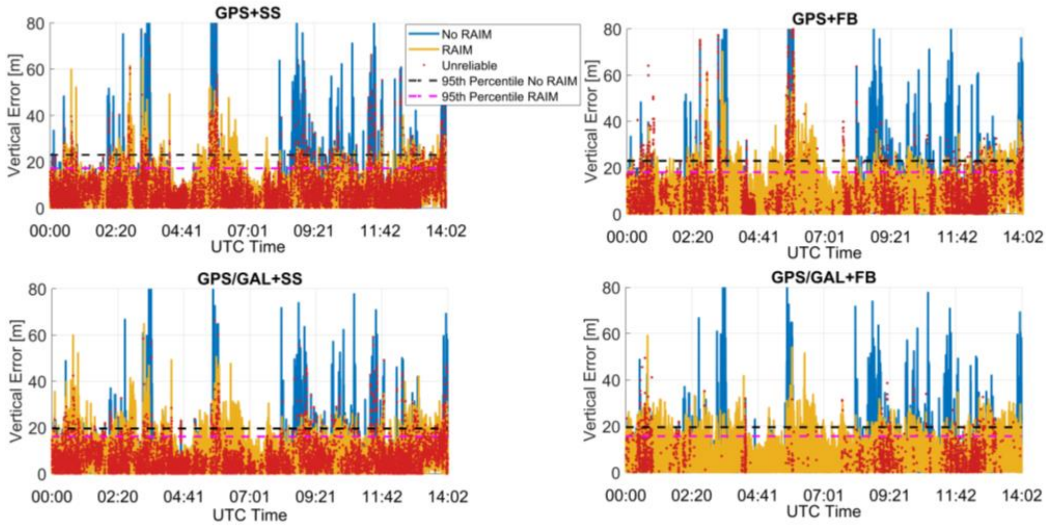

Figure 4. Vertical error as a function of time for all the considered configurations.

The reliable availability (or reliability) of the adopted configurations is shown is Figure 5, where the blue bars indicate the percentage of reliable solutions, and the yellow bars indicate the percentage of unreliable solutions. The "unreliable" solutions pertain to the following cases:

- Insufficient redundancy;
- Failure of the geometry check executed before and after the application of RAIM;
- Exceeding the horizontal and vertical alarm limits;
- The failure of the RAIM statistical tests (which, in this study, was the main cause of the solutions unreliability).

As can be seen from Figure 5, both in single and dual constellations, the FB algorithm provided better reliability (89.58% for GPS and 96.28% for GPS/Galileo). The RAIM Subset cases reached a reliable availability of 70.43% for GPS and 82.28% for GPS/Galileo, probably because of the drawback that characterizes this algorithm. The Subset scheme, in the presence of an high number of measurements, is not able to find a unique subset passing the GT.

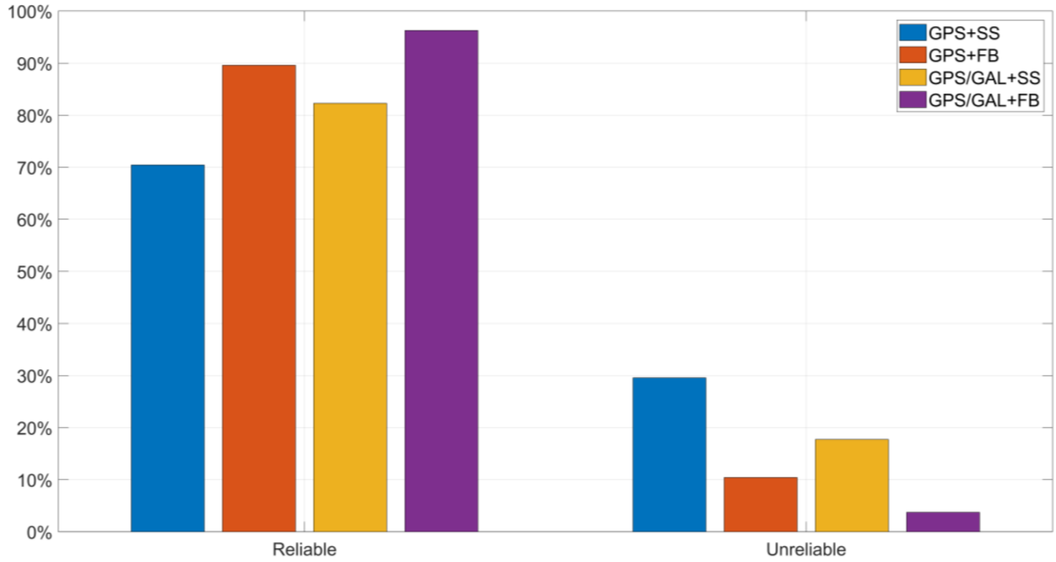

Figure 5. Reliable availability for all the considered configurations.

In order to better evaluate the performance of the used integrity algorithms, Figure 6 reports the maximum residual distribution with and without RAIM (on the left) and Cumulative Distribution Function (CDF) (right boxes) for the four considered configurations. It is important to specify that, for such graphics, the absolute value of maximum residuals vector $\underline{r}$, calculated as in (4), is considered. The residual distribution is closer to zero and with a reduced variation in the Forward–Backward case both in single and dual constellations, as also confirmed by CDF. Minor but present improvements can be noticed also for the Subset case, whose CDF is closer to the no RAIM case, showing its minor effectiveness in this test.

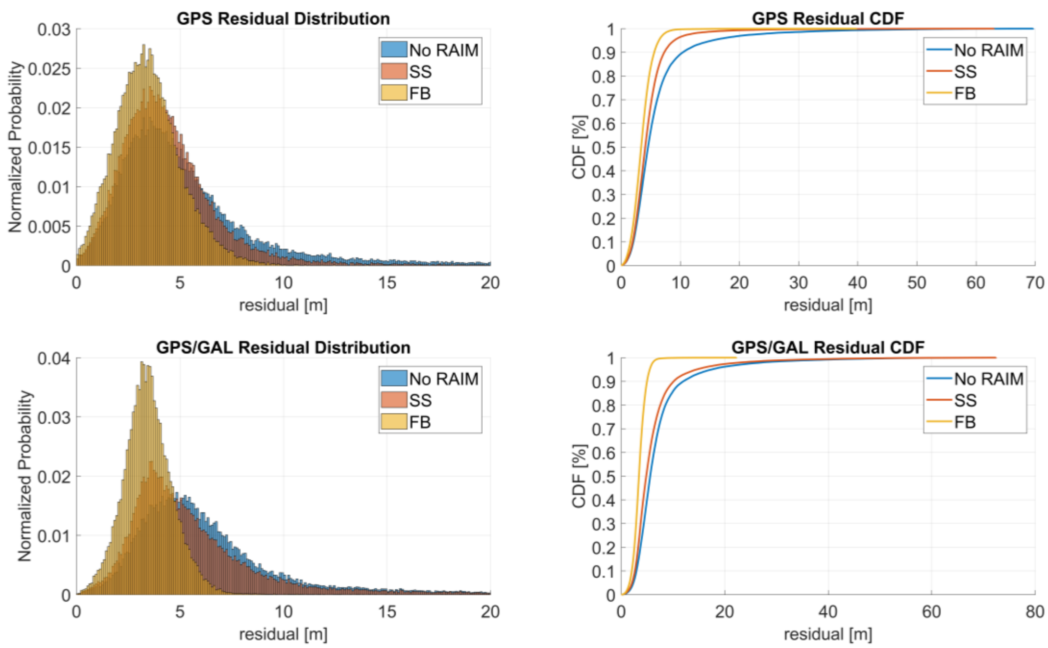

Figure 6. Residual distribution (**on the left**) and CDF (**on the right**) for all the adopted configurations.

5. Conclusions

This study involved analyzing the performance of two traditional RAIM algorithms (i.e., Subset and Forward–Backward) on the positioning of a smartphone in an obstructed environment in static mode. About 14 hours of data were processed, with and without the application of RAIM, for a total of six configurations, including GPS and Galileo measurements. From the test, it emerged that RAIM benefits are evident in difficult scenarios thanks to the exclusion of blunder-affected measurements. For the SS algorithm, a high number of unreliable solutions were observed. In the performed test, better results were provided by the FB algorithm due to its higher reliability percentage and lower horizontal and vertical errors.

Possible extensions of this study could involve simultaneous comparisons of different devices and the adoption of additional integrity algorithms.

Author Contributions: Conceptualization, A.A., G.C., S.D.P., S.G., C.G. and G.P.; methodology, A.A., G.C., S.D.P., S.G., C.G. and G.P.; software, A.A., G.C., S.D.P., S.G., C.G. and G.P.; validation, A.A., G.C., S.D.P., S.G., C.G. and G.P.; formal analysis, A.A., G.C., S.D.P., S.G., C.G. and G.P.; investigation, A.A., G.C., S.D.P., S.G., C.G. and G.P.; resources, A.A., G.C., S.D.P., S.G., C.G. and G.P.; data curation, A.A., G.C., S.D.P., S.G., C.G. and G.P.; writing—original draft preparation, A.A., G.C., S.D.P., S.G., C.G. and G.P.; writing—review and editing, A.A., G.C., S.D.P., S.G., C.G. and G.P.; visualization, A.A., G.C., S.D.P., S.G., C.G. and G.P.; supervision, A.A., G.C., S.D.P., S.G., C.G. and G.P. All authors have read and agreed to the published version of the manuscript.

Funding: This research received no external funding.

Institutional Review Board Statement: Not applicable.

Informed Consent Statement: Not applicable.

Data Availability Statement: The data presented in this study are available on request from the corresponding author.

Conflicts of Interest: The authors declare no conflict of interest.

References

1. European Union Agency for the Space Programme (EUSPA). GNSS Raw Measurements Delivering Greater Accuracy. Available online: https://www.euspa.europa.eu/newsroom/news/gnss-raw-measurements-delivering-greater-accuracy (accessed on 3 May 2023).
2. GPS World. Google Opens up GNSS Pseudoranges. Available online: https://www.gpsworld.com/google-opens-up-gnss-pseudoranges/ (accessed on 3 May 2023).
3. Zhang, X.; Tao, X.; Zhu, F.; Shi, X.; Wang, F. Quality assessment of GNSS observations from an Android N smartphone and positioning performance analysis using time-differenced filtering approach. *GPS Solut.* **2018**, *22*, 70. [CrossRef]
4. Lambert, W.; Anja, H. GNSS code and carrier phase observations of a Huawei P30 smartphone: Quality assessment and centimeter-accurate positioning. *GPS Solut.* **2020**, *24*, 64.
5. Robustelli, U.; Paziewski, J.; Pugliano, G. Observation Quality Assessment and Performance of GNSS Standalone Positioning with Code Pseudoranges of Dual-Frequency Android Smartphones. *Sensors* **2021**, *21*, 2125. [CrossRef] [PubMed]
6. Angrisano, A.; Gaglione, S. Smartphone GNSS performance in an urban scenario with RAIM application. *Sensors* **2022**, *22*, 786. [CrossRef] [PubMed]
7. Angrisano, A.; Gaglione, S.; Gioia, C. RAIM algorithms for aided GNSS in urban scenario. In Proceedings of the 2012 Ubiquitous Positioning, Indoor Navigation, and Location Based Service (UPINLBS), Helsinki, Finland, 3–4 October 2012; pp. 1–9.
8. ESA Navipedia. RAIM. Available online: https://gssc.esa.int/navipedia/index.php/RAIM#RAIM_Concept (accessed on 3 May 2023).
9. Kaplan, E.D.; Hegarty, C.J. *Understanding GPS. Principles and Applications*, 2nd ed.; Artech House: Norwood, MA, USA, 2006.
10. Teunisses, P.J.; Montenbruck, O. *Springer Handbook of Global Navigation Satellite Systems*; Springer International Publishing: Cham, Switzerland, 2017.
11. Zishen, L.; Liang, W.; Ningbo, W.; Ran, L.; Ang, L. Real-time GNSS precise point positioning with smartphones for vehicle navigation. *Satell. Navig.* **2022**, *3*, 19.
12. Amarildo, H.; Harris, P.; Thanassis, M.; Vassilis, G. Testing of a Combined Hatch Filter / RAIM Algorithm for SPP Smartphone Kinematic Positioning in GNSS Harsh Environments. In Proceedings of the 2nd Symposium of IAG Commission 4 "Positioning and Applications", Potsdam, Germany, 5–8 September 2022.
13. EUSPA—European Union Agency for the Space Programme. «World's First Dual-Frequency GNSS Smartphone Hits the Market» 2018. Available online: https://www.euspa.europa.eu/newsroom/news/world-s-first-dual-frequency-gnss-smartphone-hits-market (accessed on 15 May 2023).
14. Parkinson, B.W.; Spilker, J.J.J. *Global Positioning System: Theory and Applications*; American Institute of Aeronautics and Astronautics, Inc.: Reston, VA, USA, 1996.

15. Kuusniemi, H. User-Level Reliability and Quality Monitoring in Satellite-Based Personal Navigation. Ph.D. Thesis, Tampere University of Technology, Tampere, Finland, 2005.
16. Kuusniemi, H.; Wieser, A.; Lachapelle, G.; Takala, J. User-level reliability monitoring in urban personal satellite navigation. *IEEE Trans. Aerosp. Electron. Syst.* **2007**, *43*, 1305–1318. [CrossRef]
17. Angrisano, A.; Gioia, C.; Gaglione, S.; Del Core, G. GNSS Reliability Testing in Signal-Degraded Scenario. *Int. J. Navig. Obs.* **2013**, *2013*, 870365. [CrossRef]
18. Chin, G.Y.; Kraemer, J.H.; Brown, R.G. GPS RAIM: Screening Out Bad Geometries Under Worst-Case Bias Conditions. *Navigation* **1992**, *39*, 407–427. [CrossRef]
19. Xiaomi. About Us. Available online: https://www.mi.com/global/about/ (accessed on 29 November 2023).
20. Broadcom. Company History. Available online: https://www.broadcom.com/company/about-us/company-history (accessed on 29 November 2023).